Lectures on Bound states in gauge theory

Paul Hoyer
Department of Physics and Helsinki Institute of Physics
POB 64, FIN-00014 University of Helsinki, Finland

Hadrons are successfully classified in terms of the properties of non-relativistic $q\bar{q}$ and qqq bound states. This is remarkable, since relativistic states do not have a fixed number of constituents, nor are the quark spins and orbital angular momenta separately conserved. For heavy quarkonia even the spectra are strikingly similar to those of atoms. Motivated by these and related observations we recall in these lectures the physics of QED bound states and the derivation of atoms from first principles in QED. The aim is to scrutinize whether any possibility exists to apply analogous and rigorous methods to relativistic hadrons, taking into account their novel features of confinement and chiral symmetry breaking.
Bound state poles in QED amplitudes are generated by the divergence of an infinite sum of Feynman diagrams. The sum is required because one perturbs around free (*in* and *out*) electrons, unaccompanied by their electromagnetic fields. In effect, the sum of ladder diagrams builds the atomic $-\alpha/r$ potential required by the field equations of motion. In QCD, without the guidance of an expansion in α_s, we do not know how to perform such a summation. However, any sum should give a field that is consistent with the equations of motion and Poincaré invariance. This allows the addition of a linear Coulomb field for neutral states, which could be relevant for QCD.
After a brief review of high precision calculations of atomic spectra I show explicitly how the Schrödinger equation is obtained at lowest order in the atomic rest frame. This is then generalized to a frame where the atom is in relativistic CM motion. Equal time wave functions have a dynamical frame dependence, which provides a quantum analog of classical Lorentz contraction. From the sum of Feynman diagrams that generate the Dirac equation we see that Dirac bound states of an electron include Fock states with any number of e^+e^- pairs. The meaning of the apparently single electron Dirac wave function is illuminated by considering the bound state as an eigenstate of the Hamiltonian. This also helps to understand why the solutions of the Dirac equation in a linear potential cannot be normalized, a fact that has been known for a long time but largely ignored.
...

Contents

I. INTRODUCTION

Bound state physics is omitted from many textbooks on relativistic field theory. Introductory courses in quantum mechanics, on the other hand, typically begin by postulating the Schrödinger equation, and then solve it for atomic wave functions and binding energies. The wave functions depend exponentially on the fine structure constant α, the small parameter of QED perturbation theory. While scattering amplitudes typically are calculated from Feynman diagrams order by order in α, we need to sum an infinite series of diagrams to find bound states. One of the aims of these lectures is to clarify the physical reason for this feature of bound state calculations.

The Schrödinger equation gives only the lowest order (in α) approximation of atomic binding energies. In 1951 Salpeter and Bethe [1] derived a formally exact and Poincaré covariant bound state equation, which has formed the basis of many calculations of atomic spectra [2]. The Bethe-Salpeter wave function of, *e.g.*, a positronium bound state $|e^+e^-, P\rangle$ that has CM momentum P is defined as

$$\Phi^P_{\alpha\beta}(x_1 - x_2)e^{-iP\cdot(x_1+x_2)/2} \equiv \langle\Omega|\ T\left\{\bar\psi_\beta(x_2)\psi_\alpha(x_1)\right\}\left|e^+e^-, P\right\rangle \tag{1.1}$$

where $\psi(x)$ is the electron field operator and $|\Omega\rangle$ is the vacuum state. The trivial dependence on $x_1 + x_2$ is specified by translation invariance since the bound state is a momentum eigenstate, $P = (\sqrt{M^2 + \boldsymbol{P}^2}, \boldsymbol{P})$. The positronium state can be expanded in terms of its complete set of Fock states

$$|P\rangle = \int d^3\boldsymbol{x}_1\, d^3\boldsymbol{x}_2\, \phi^P_{e^+e^-}(\boldsymbol{x}_1, \boldsymbol{x}_2)\left|e^+e^-, P\right\rangle + \int d(\cdots)\phi^P_{e^+e^-\gamma}(\cdots)\left|e^+e^-\gamma, P\right\rangle + \ldots \tag{1.2}$$

Since the Heisenberg and Schrödinger pictures merge at $t = 0$ the Fock wave functions ϕ are equal-time wave functions. Correspondingly, the Bethe-Salpeter wave function (1.1) equals the e^+e^- Fock state wave function $\phi^P_{e^+e^-}$ when $x^0_1 = x^0_2$.

The Bethe-Salpeter equation (BSeq) is in momentum space of the form

$$\Phi(p) \equiv \int d^4x\, \Phi(x)e^{ip\cdot x} = S(p)\int \frac{d^4q}{(2\pi)^4}\ K(p,q)\ \Phi(q) \tag{1.3}$$

where $S(p)$ is a two-particle propagator and K is the interaction kernel. By iterating this equation one obtains contributions with higher powers of K and thus of α. At lowest order the kernel K is given by single photon exchange.

It turned out to be difficult in practice to calculate higher order corrections to bound state energies from the BSeq (1.3). The wave function cannot be expressed in closed form even when only the lowest order kernel is used. However, because the equation involves *two* functions S and K, there is a freedom in choosing either one, without affecting the validity of the equation [3]. This is seen as follows.

Let G_T be the Green function for a $2 \to 2$ scattering process with the external propagators truncated. The perturbative expansion of G_T in α may be calculated using the standard Feynman rules. We then define a Dyson-Schwinger type equation by

$$G_T = K + K\,S\,G_T \tag{1.4}$$

where the products imply convolutions over four-momenta similar to that in (1.3). This equation is valid provided the kernel satisfies

$$K = G_T\,(1 + S\,G_T)^{-1} = G_T - G_T\,S\,G_T + ... \tag{1.5}$$

Thus the "propagator" S may in fact be chosen freely. The expansion of K in α follows from the expansions of S and G_T. The non-truncated Green function G is given by

$$G \equiv S + S\,G_T\,S = S + S\,K\,G \tag{1.6}$$

As a consequence of unitarity the residues of the bound state poles of G factorize into a product of wave functions for the initial and final state (Fig. 1),

$$G \to \frac{\Phi_n\bar\Phi_n}{P^0 - E_n} \quad \text{as} \quad P^0 \to E_n \tag{1.7}$$

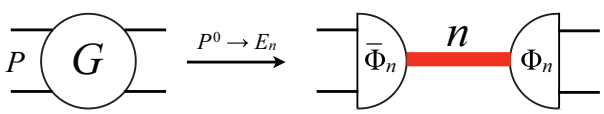

FIG. 1: Bound states appear as poles in scattering amplitudes. Unitarity requires that the residue factorizes into a product of incoming and outgoing wavefunctions.

where P is the CM momentum of the bound state and E_n its energy. Substituting (1.7) into (1.6) the BSeq (1.3) follows. With a suitable choice of the propagator S analytic expressions for the wave functions are obtained

when the lowest order kernel is used in the BSeq. These solutions facilitate calculations of higher order corrections to the binding energies [2].

The wide range of possibilities in the choice of a BSeq motivated a search for an optimal approach selected by physical arguments. The perturbative expansion relies on the non-relativistic nature of atoms, $v/c \simeq \alpha \ll 1$. This suggested the use of an effective QED Lagrangian called NRQED [4], which is essentially an expansion of the standard Lagrangian in powers of p/m_e. At the expense of introducing more interactions the NRQED Lagrangian allows to use non-relativistic dynamics, which is of great help in high order calculations [5]. The probability of finding high relative momenta, $p \sim m_e$, in positronium was estimated to be $\alpha^5 \sim 10^{-11}$, making NRQED very efficient.

The continuous development of theoretical and experimental techniques have allowed precision tests of QED using bound states. For example, the energy difference ΔE between orthopositronium ($J^{PC} = 1^{--}$) and parapositronium ($J^{PC} = 0^{-+}$), expressed in terms of $\Delta\nu \equiv \Delta E/2\pi\hbar$, is calculated using NRQED methods to be [6]

$$\begin{aligned}\Delta\nu_{QED} \;=\; & m_e\alpha^4\left\{\frac{7}{12}-\frac{\alpha}{\pi}\left(\frac{8}{9}+\frac{\ln 2}{2}\right)\right. \\ & +\frac{\alpha^2}{\pi^2}\left[-\frac{5}{24}\pi^2\ln\alpha+\frac{1367}{648}-\frac{5197}{3456}\pi^2+\left(\frac{221}{144}\pi^2+\frac{1}{2}\right)\ln 2-\frac{53}{32}\zeta(3)\right] \\ & \left.-\frac{7\alpha^3}{8\pi}\ln^2\alpha+\mathcal{O}\left(\alpha^3\ln\alpha\right)\right\} = 203\,392.01 \pm 0.46 \text{ MHz}. \end{aligned} \tag{1.8}$$

which is about $3\,\sigma$ from the experimental value, $\Delta\nu_{EXP} = 203\,389.10 \pm 0.74$ MHz [7]. The appearance of $\ln\alpha$ in (1.8) demonstrates that bound state perturbation theory indeed differs from the usual expansions of scattering amplitudes.

The successes of QED have inspired the use of analogous methods for the other interactions. In particular, Bethe-Salpeter and Dyson-Schwinger equations have been extensively applied in QCD [8]. Viewed as non-perturbative equations they give exact relations between Green functions but do not close – an infinite set of functions are coupled to each other. Models based on judicious truncations have allowed studies of spontaneous chiral symmetry breaking and been successfully compared to hadron properties deduced from data and lattice calculations.

Effective theories analogous to NRQED have been formulated for heavy quarks with mass $m_Q \gg \Lambda_{QCD}$, and used to describe $Q\bar{Q}$ bound states [9]. These methods are applicable in the limit where the quarkonia have small enough radius for perturbative gluon exchange to dominate over the confining interaction.

The aim of these lectures is foremost to gain a basic understanding of bound state physics through QED: Why do we need to sum an infinite set of Feynman diagrams? Which diagrams sum to the Schrödinger equation, and how do we get the Dirac equation? Is it conceivable that we could apply analogous methods to hadrons, the relativistic bound states of QCD? Our only first-principles (model independent) approach to hadrons is presently provided by numerical lattice gauge theory. As shown in Fig. 2 [10], lattice calculations have been very successful, demonstrating that QCD also describes soft hadronic phenomena.

Color confinement and the emergence of the physical scale Λ_{QCD} in QCD are novel features which do not appear in QED atoms. Nevertheless, the observed hadron spectrum has remarkable similarities with atoms, as shown for charmonia in Fig. 3. The quark model gives a quantitative description of charmonia and bottomonia using the non-relativistic Schrödinger equation with the potential

$$V(r) = c\,r - \frac{4}{3}\frac{\alpha_s}{r} \tag{1.9}$$

The linear term should arise from non-perturbative physics, while the $1/r$ potential corresponds to single gluon (perturbative) exchange. Also light hadrons can be classified in terms of just their valence ($q\bar{q}$ or qqq) degrees of freedom, despite their relativistic nature and sea quark constituents.[1].

Comparisons like that of Fig. 3 as well as a number of other striking properties of hadrons, including duality and the OZI rule (to be discussed below), motivate a careful analysis of bound states in QED. Is there any

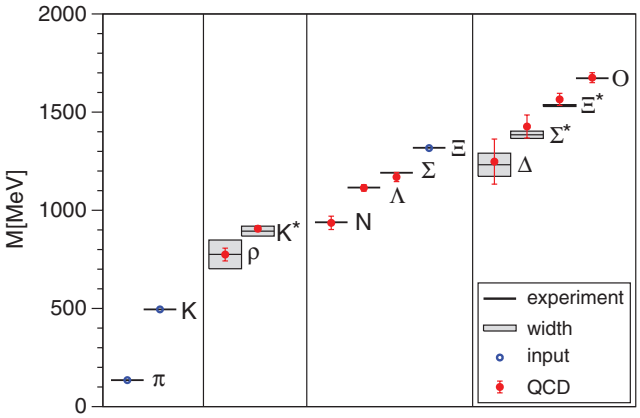

FIG. 2: The light hadron spectrum of QCD. Horizontal lines and bands are the experimental values with their decay widths. The QCD lattice results [10] are shown by solid circles. Vertical error bars represent the combined statistical and systematic error estimates. π, K, and Ξ have no error bars, because they are used to set the light quark mass, the strange quark mass, and the overall scale, respectively.

[1] Hadrons also bind to form nuclei and other molecular-type states, in analogy to the molecules of QED.

way that a confining potential like that in (1.9) could arise in a less *ad hoc* way, consistently with the rules of field theory?

We begin by reviewing how bound state poles in scattering amplitudes arise through the divergence of the perturbative series. "Ladder diagrams" of any order in α must be taken into account, no matter how small is α. This is because perturbation theory expands around states with free electrons, unaccompanied by an electromagnetic field. Such states are unphysical in the sense that they do not satisfy the field equations of motion. The sum of ladder diagrams in effect rebuilds the missing classical $-\alpha/r$ potential. On the other hand, the Schrödinger equation follows directly when the Hamiltonian operates on an e^+e^- state with an A^0 field that satisfies Gauss' law.

The binding energy of positronium is at lowest order $E_B = -\frac{1}{2}\mu\alpha^2 \simeq 6.8$ eV ($\mu = m_e/2$ is the reduced mass). This is a tiny fraction of $2m_e$, the approximate mass of positronium. QED calculations such as that of (1.8) make use of the weak atomic binding ($\alpha \ll 1$). By contrast, hadron binding energies are characterized by the scale $\Lambda_{QCD} \sim 200$ MeV which is much larger than the light quark masses ($m_u,\ m_d \sim \mathcal{O}(10)$ MeV). The excitation energies of light hadrons are therefore commensurate with the hadron masses[2].

How can we obtain information on strongly bound (relativistic) bound states from QED, given that $\alpha \ll 1$? We discuss two instructive cases below:

(i) We consider positronium in a frame where its CM momentum is relativistic. Even though the *relative* (transverse) momentum of the electron and positron remains of $\mathcal{O}(\alpha m)$ (the Bohr momentum), they move relativistically together along the positronium line of flight. Surprisingly, the equal-time wave function of positronium in motion was derived only recently [12]. This question is of more general interest as it demonstrates how the Lorentz contraction familiar from classical relativity manifests itself (non-trivially) in quantum physics.

(ii) The Dirac equation determines the binding energies of a relativistic electron in an external field, generated by a fixed charge Ze. Dirac bound states are given by the sum of all Feynman diagrams that are of leading power in $Z\alpha$, in the infinite mass limit of the particle with charge Ze. In contrast to the non-relativistic case, all crossed ladders must be included [13]. This implies that the Dirac state has Fock components with any number of e^+e^- pairs. Consequently the Dirac wave function does not describe just a single electron, even though it has a single argument. As was realized already in the 1930's [14] but is now largely forgotten, for a linear potential the Dirac wave function is not normalizable and the spectrum is continuous.

The Hamiltonian formulation of positronium and Dirac bound states can be generalized to translation-invariant, relativistic bound states. We study their properties in $D = 1 + 1$ dimensions, where the QED Coulomb potential $V(x)$ is linear. The spectrum is discrete and has a novel type of boost covariance. The energy E depends on the

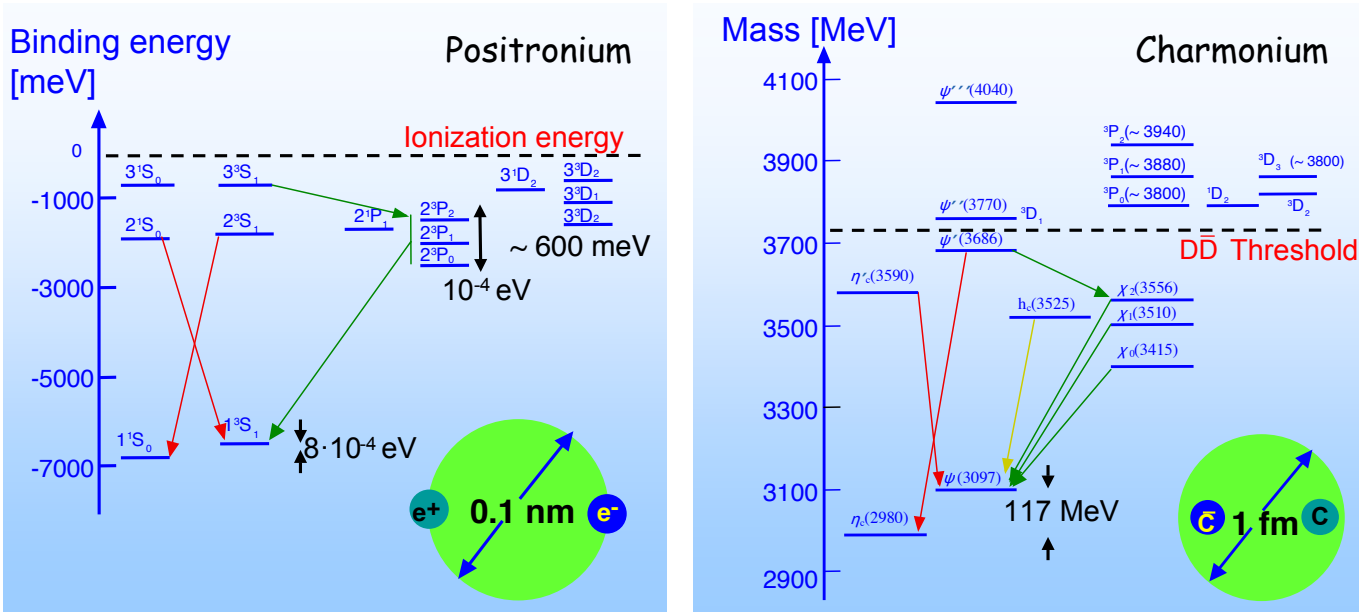

FIG. 3: Comparison of atomic (positronium) and hadronic (charmonium) spectra [11]. Their similarity, despite the $\mathcal{O}(10^9)$ difference in energy scale, suggests to study whether QCD hadrons might be described analogously to QED atoms.

[2] The excitation energies are large compared to $m_u,\ m_d$ also for the charmonia of Fig. 3. Nevertheless, the light quark degrees of freedom do not appear to be important for the description of charmonia.

momentum P as imposed by Lorentz invariance, $E = \sqrt{M^2 + P^2}$, and the wave function Lorentz contracts according to the kinetic (as opposed to canonical) energy, $\propto 1/(E - V)$. The Poincaré invariance allows to determine bound state scattering amplitudes. The parton distribution determined from Deep Inelastic Scattering has a "sea-quark" type enhancement at small x_{Bj}.

There is no obvious, first-principles method of summing Feynman diagrams to obtain relativistic bound states like hadrons. In the absence of a hierarchy in the magnitudes of the diagrams a model-dependent truncation is required. However, an indirect method appears possible: The instantaneous A^0 field associated with a given charge configuration should satisfy Gauss' law. In addition to the usual $1/r$ potential In $D = 3 + 1$ dimensions there are also homogeneous solutions corresponding to a non-vanishing field strength at spatial infinity. The only such potential which is compatible with Poincaré invariance is linear, and requires the bound state to be neutral. This type of solution can be applied to $q\bar{q}$ mesons and qqq baryons of QCD. Its possible relevance to the experimentally observed hadrons is a tantalizing possibility.

II. POSITRONIUM FROM FEYNMAN DIAGRAMS

A. The divergence of the perturbative expansion caused by bound states

On general grounds we know that bound states appear as poles in scattering amplitudes. The poles are on the real axis of the complex energy plane for stable bound states (like protons) and below the real axis in case of unstable states. It is perhaps worthwhile to illustrate this using the free scalar propagator

$$D(p^0, \boldsymbol{p}) = \frac{i}{p^2 - m^2 + i\varepsilon} \tag{2.1}$$

Fourier transforming $p^0 \to t$,

$$D(t, \boldsymbol{p}) \equiv \int \frac{dp^0}{2\pi} D(p^0, \boldsymbol{p}) \exp[-ip^0 t] = \frac{1}{2E_p}\left[\theta(t)e^{-iE_p t} + \theta(-t)e^{iE_p t}\right] \tag{2.2}$$

where $E_p = \sqrt{\boldsymbol{p}^2 + m^2}$. We see that in the reverse transformation $t \to p^0$ the poles of (2.1) in p^0 are created by the infinite range of the t-integration.

By definition, bound states are stationary in time,

$$H\,|P,t\rangle = P^0\,|P,t\rangle \quad \Longrightarrow \quad |P,t\rangle = e^{-iP^0 t}\,|P,0\rangle \tag{2.3}$$

with $P^0 = \sqrt{\boldsymbol{P}^2 + M^2}$. The bound state contribution to a completeness sum in an amplitude $\langle f, t_f | i, t_i\rangle$ with $E_i = E_f = P^0$ will then be

$$\langle f, t_f|\,|P,t\rangle\,\langle P,t|i,t_i\rangle = \langle f|P\rangle e^{-i(t_f - t_i)P^0}\langle P|i\rangle \tag{2.4}$$

The Fourier transform $t_f - t_i \to p^0$ will generate a pole at $p^0 = P^0$, with residue equal to a product of the initial $\langle P|i\rangle$ and final state wave functions, as already indicated in (1.7) and Fig. 1. This holds for any bound state, no matter how complicated.

The rest frame ($\boldsymbol{P} = 0$) energies of positronium bound states are

$$P^0 = 2m_e + E_B \tag{2.5}$$

with binding energies $E_B = -\frac{1}{4}m_e\alpha^2/n^2 \simeq -6.8\ \mathrm{eV}/n^2$ (at lowest order in α, with $n = 1, 2, \ldots$). Hence the elastic e^+e^- amplitude $G(e^+e^- \to e^+e^-)$ has an infinite set of positronium poles just below threshold ($s = E_{CM}^2 = 4m_e^2$), and slightly below the real s-axis due to the finite life-times. How are these poles generated by the Feynman diagrams describing G?

We may regard the positions of the bound state poles at $s = (2m_e + E_B)^2$ as functions of E_B, *i.e.*, of α. It is then clear that no Feynman diagram of finite order in α can have such a pole. The only way to generate a bound state pole in G is for the perturbative expansion to diverge![3] This sounds surprising at first, since we are used to trusting QED perturbation theory, and the poles exist for any α, however small. Thus some higher order diagrams, such as those in Fig. 4, must contribute at the same level as the Born term (a).

---

[3] This divergence is distinct from that due to perturbative expansions being generally asympototic [15].

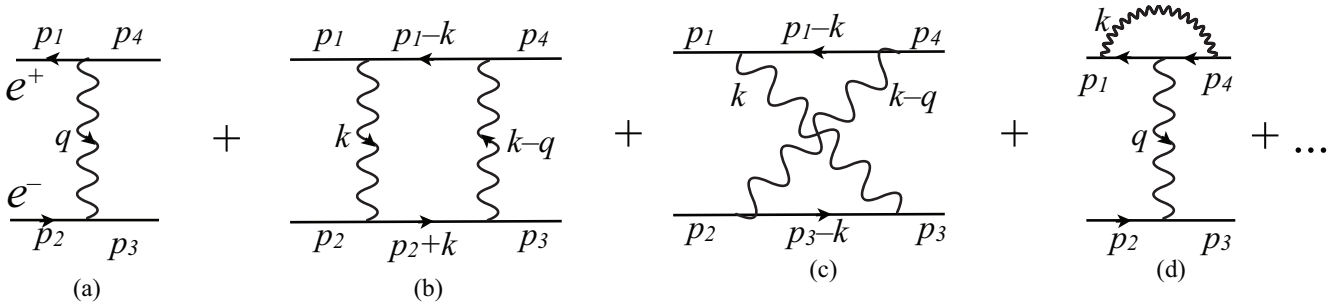

FIG. 4: Feynman diagrams contributing to elastic $e^+(p_1)e^-(p_2)$ scattering. The arrows indicate the fermion direction. The momentum of the upper line is in the antifermion (e^+) direction, thus $p_1^0 > 0$.

The breakdown of the perturbative expansion is actually familiar from classical physics, where phenomena involving many photons dominate. For example, the notion that opposite charges attract while like charges repel cannot be explained by just the Born term in Fig. 4. This diagram only changes sign if $e^+ \to e^-$, so its absolute square is invariant. The product of diagrams (a) and (b), on the other hand, contributes with opposite signs to $\sigma(e^\pm e^- \to e^\pm e^-)$. Thus our everyday experience of attraction and repulsion originates from quantum interference effects.

Higher order diagrams have not only more vertices $\propto e$ but also more propagators, which are enhanced at low momenta. In atoms the momentum exchanges are of the order of the Bohr momentum, and energy differences follow from non-relativistic dynamics:

$$|\boldsymbol{q}| \sim \alpha m_e \qquad\qquad q^0 \sim \boldsymbol{q}^2/2m_e \sim \tfrac{1}{2}\alpha^2 m_e \tag{2.6}$$

The Born diagram in Fig. 4 scales with α as

$$G[4(a)] \sim \alpha/q^2 \sim \alpha/\boldsymbol{q}^2 \sim 1/\alpha \tag{2.7}$$

The box diagram 4(b) has two photon exchanges, each of $\mathcal{O}\left(\alpha^{-2}\right)$. The electron and positron propagators are off-shell on the order $q^0 \sim k^0$, each propagator being of $\mathcal{O}\left(\alpha^{-2}\right)$. The relevant region of loop momentum is $\int dk^0\, d^3\boldsymbol{k} \sim \alpha^2\,(\alpha)^3 \sim \alpha^5$. Together with the four vertices this gives

$$G[4(b)] \sim \alpha^2\,\alpha^5\,(\alpha^{-2})^2\,(\alpha^{-2})^2 \sim 1/\alpha \tag{2.8}$$

A similar analysis shows that "ladder" diagrams with any number of photon exchanges are of $\mathcal{O}\,(1/\alpha)$ and thus of the same order in α as the Born diagram (2.7). This allows the perturbative series to diverge for any α. Note that the above counting requires the initial and final momenta $p_1, \ldots p_4$ of the scattering to themselves satisfy the scaling (2.6): If $\alpha \to 0$ the external momenta need to be correspondingly adjusted. Conversely, in a "hard" scattering process where the momentum exchange $|\boldsymbol{q}| \gg \alpha m_e$ the initial and final states do not couple to the bound states, $\langle P|i\rangle \sim \langle f|P\rangle \simeq 0$ in (2.4), and bound state contributions can be ignored. In the following we shall see more such analogies to "hard" and "soft" processes in QCD. In QED we know how to deal with "soft" scattering, which may be helpful for understanding the properties of QCD.

All except the ladder diagrams scale with a higher power of α than the Born term, and can thus be ignored in a lowest order calculation of non-relativistic bound states. We shall not prove this, but just illustrate by the crossed ladder (c) and the vertex correction (d) in Fig. 4. Both have the same number of propagators and vertices as the straight ladder (b), and would give the same estimate as in (2.8). However, their leading contributions cancel in the loop integration. Since $-p_1^0 = -m_e + \mathcal{O}\left(\alpha^2\right)$ whereas $p_3^0 = +m_e + \mathcal{O}\left(\alpha^2\right)$, the leading contribution comes from the negative energy pole in the $(-p_1 + k)$ propagator, and from the positive energy pole in the $(p_3 - k)$ propagator. The Feynman $i\varepsilon$ prescription implies that both poles are in the $\mathrm{Im}k^0 > 0$ hemisphere. Closing the k^0 contour in the $\mathrm{Im}k^0 < 0$ plane these poles do not contribute. The situation is similar for the vertex diagram (d), whereas for the straight ladder (b) the integration contour is pinched by the two poles.

B. Bound state Born terms

The concept of "Born term" is useful for scattering amplitudes: It is the lowest order contribution, given by one or several tree diagrams. Born terms are unique and semi-classical in the sense that they are of lowest order in $\hbar$, they are Poincaré covariant and typically give a good first approximation of the scattering amplitude. Each loop correction brings an additional power of $\hbar$ [16]. The Schrödinger equation gives the lowest order approximation to atoms, so in this sense its solutions are the Born terms of atomic bound states. Whether they may also be regarded as of lowest

order in $\hbar$ requires further discussion, since bound states are generated by loop (ladder) diagrams. We shall briefly review the arguments of [17] here, since the Born term concept may allow an objective definition of a lowest order approximation to relativistic bound states.

We usually expect to recover classical physics in the $\hbar \to 0$ limit. This would exclude bound states, which are quantum phenomena. The outcome turns out to depend on how the limit is defined: Which other variables are held fixed in the limit? The situation is similar to what we found in (2.7) and (2.8) for the $\alpha \to 0$ limit of ladder diagrams, which had a leading behavior $\sim 1/\alpha$ provided the external momenta scaled with α.

The standard harmonic oscillator with potential $V(x) = \frac{1}{2}m\omega^2 x^2$ illustrates how the result depends on the definition of the $\hbar \to 0$ limit. The amplitude for the propagation of a particle from (t_i, x_i) to (t_f, x_f) is given by the path integral

$$\mathcal{A}(x_i, x_f; t_f - t_i) = \int [\mathcal{D}x(t)] \exp\left[\frac{im}{2\hbar}\int_{t_i}^{t_f} dt(\dot{x}^2 - \omega^2 x^2)\right] = \int [\mathcal{D}\xi(t)] \exp\left[\frac{im}{2}\int_{t_i}^{t_f} dt(\dot{\xi}^2 - \omega^2\xi^2)\right] \tag{2.9}$$

In the second equality the explicit dependence on $\hbar$ was removed by scaling the coordinates as $\xi \equiv x/\sqrt{\hbar}$. The full quantum mechanical structure of the harmonic oscillator model persists as $\hbar \to 0$ provided the variables ξ are held fixed. In other words, there is a domain of positions $x \propto \sqrt{\hbar}$ and momenta $m\dot{x} \propto \sqrt{\hbar}$ where the action S is proportional to $\hbar$ and the system stays quantum mechanical even in the $\hbar \to 0$ limit. If alternatively the positions x_i, x_f are considered to be independent of $\hbar$ then $\xi_i, \xi_f \propto 1/\sqrt{\hbar}$ grow large, and the transitions between highly excited levels is described by classical dynamics.

Consider now QED, which has the dimensionless coupling $\alpha = e^2/(4\pi\hbar)$. Curiously, if we keep the classical charge e fixed as $\hbar \to 0$ we find $\alpha \propto 1/\hbar \to \infty$. Such a scaling does not give a factor $\hbar$ for each loop, as was demonstrated by Holstein and Donoghue [18]).

Let us do a standard dimensional analysis of the QED fields, keeping explicitly the powers of $\hbar$. The dimension of the action is $[S] \sim \hbar \sim E\,L$, where E is a unit of energy (or momentum, since $c = 1$) and L is a unit of length (or time). From the kinetic part of the QED action $\int d^4x \bar{\psi}\, i\partial\!\!\!/\, \psi$ follows that the fermion field has dimension $[\psi] \sim E^{1/2}\, L^{-1}$. The gauge field action $-\frac{1}{2}\int d^4x\, F_{\mu\nu}F^{\mu\nu}$ requires that $[A^\mu] \sim E^{1/2}\, L^{-1/2}$. The mass term in the QED action must then be written $\int d^4x \bar{\psi}(m/\hbar)\psi$ since $[m] \sim E$. Finally, the interaction term $\int d^4x \bar{\psi}(e/\hbar)A\!\!\!/\psi$ also needs a factor $1/\hbar$.

In order to eliminate the factor $\hbar$ in the weight $\exp(iS/\hbar)$ of the functional integral we may rescale the fields, similarly as for the Harmonic Oscillator in (2.9):

$$\tilde{\psi} = \psi/\sqrt{\hbar} \qquad\qquad \tilde{A}^\mu = A^\mu/\sqrt{\hbar} \tag{2.10}$$

Then provided

$$\tilde{m} = m/\hbar \qquad\qquad \tilde{e} = e/\hbar \tag{2.11}$$

are kept fixed as $\hbar \to 0$ only the interaction term retains an $\hbar$. The functional integral becomes

$$Z = \int [\mathcal{D}\bar{\tilde{\psi}}][\mathcal{D}\tilde{\psi}][\mathcal{D}\tilde{A}] \exp\left\{ i\int d^4x \left[\bar{\tilde{\psi}}(i\partial\!\!\!/ - \tilde{e}\sqrt{\hbar}\tilde{A}\!\!\!/ - \tilde{m})\tilde{\psi} - \tfrac{1}{4}\tilde{F}_{\mu\nu}\tilde{F}^{\mu\nu}\right]\right\} \tag{2.12}$$

Since the $\tilde{e}$ and $\hbar$ appear only in the combination $\tilde{e}\sqrt{\hbar}$ there is a strict correspondence between the powers of $\tilde{e}$ (or α) and the powers of $\hbar$ in any Green function: The loop and $\hbar$ expansions are equivalent.

Note that due to the rescaling of the fields the number of external legs affects the overall power of $\hbar$. Thus the free electron and photon propagators are of $\mathcal{O}(\hbar)$:

$$\langle\bar{\psi}\psi\rangle \sim \hbar\langle\bar{\tilde{\psi}}\tilde{\psi}\rangle \sim \hbar \qquad\qquad \langle AA\rangle \sim \hbar\langle\tilde{A}\tilde{A}\rangle \sim \hbar \tag{2.13}$$

In Section II A we found that ladder diagrams were of the same order in α as the Born term. Since the powers of α and $\hbar$ are strictly related in the limit we consider here, the ladder diagrams are also of the same order in $\hbar$ as the Born term: The concept of Born term for non-relativistic bound states makes sense, and is represented by the Schrödinger equation. The parts of the ladder diagrams where the loop momenta do not scale as in (2.6) contribute to bound states with a higher power of α and $\hbar$. Thus we see that the same Feynman diagram can contribute to scattering amplitudes at several powers of $\hbar$. In the following we return to the standard convention with $\hbar = 1$.

C. Evaluating ladder diagrams

The standard Feynman rules give for the Born diagram Fig. 4(a),

$$L_1(p_1, p_2 \to p_1 - q, p_2 + q) = \bar{v}(p_1)(-ie\gamma^\mu)v(p_4)D_{\mu\nu}(q)\bar{u}(p_3)(-ie\gamma^\nu)u(p_2) \tag{2.14}$$

The double ladder Fig. 4(b) is similarly

$$\begin{aligned} L_2(p_1,p_2\to p_1-q,p_2+q) &= \int \frac{d^4k}{(2\pi)^4}\bar v(p_1)(-ie\gamma^\mu)i\frac{-\not p_1+\not k+m}{(-p_1+k)^2-m^2+i\varepsilon}(-ie\gamma^\rho)v(p_4)\\ &\quad\times D_{\mu\nu}(k)\,D_{\rho\sigma}(k-q)\\ &\quad\times \bar u(p_3)(-ie\gamma^\sigma)i\frac{\not p_2+\not k+m}{(p_2+k)^2-m^2+i\varepsilon}(-ie\gamma^\nu)u(p_2) \end{aligned} \tag{2.15}$$

The positive and negative energy poles of a fermion propagator may be separated using the identity

$$\frac{\not p+m}{p^2-m^2+i\varepsilon}=\frac{1}{2E_p}\sum_\lambda\Big[\frac{u(\boldsymbol p,\lambda)\bar u(\boldsymbol p,\lambda)}{p^0-E_p+i\varepsilon}+\frac{v(-\boldsymbol p,\lambda)\bar v(-\boldsymbol p,\lambda)}{p^0+E_p-i\varepsilon} \tag{2.16}$$

where $E_p=\sqrt{\boldsymbol p^2+m^2}$ and $\lambda=\pm\frac12$ is the helicity. Note that on the rhs. p^0 appears only in the numerator. In the region (2.6) relevant for bound states at lowest order, k^0 in (2.15) is small compared to the fermion energy so that

$$\begin{aligned} (-p_1+k)^0 &\simeq -E_{1k}\equiv-\sqrt{(\boldsymbol p_1-\boldsymbol k)^2+m^2} &\Longrightarrow&\quad \text{keep only the } v\bar v \text{ term}\\ (p_2+k)^0 &\simeq +E_{2k}\equiv \sqrt{(\boldsymbol p_2+\boldsymbol k)^2+m^2} &\Longrightarrow&\quad \text{keep only the } u\bar u \text{ term} \end{aligned} \tag{2.17}$$

With this approximation we find

$$\begin{aligned} L_2(p_1,p_2\to p_1-q,p_2+q) &= \sum_{\lambda_{int}}\int\frac{d^4k}{(2\pi)^4}\,L_1(p_1,p_2\to p_1-k,p_2+k)\\ &\quad\times\ S(p_1-k,p_2+k)L_1(p_1-k,p_2+k\to p_1-q,p_2+q)\\ &\equiv\ L_1\,S\,L_1 \end{aligned} \tag{2.18}$$

where the convolution is over the helicities λ_{int} and momenta k of the intermediate state with propagator S,

$$S(p_1-k,p_2+k)=\frac{i}{-p_1^0+k^0+E_{1k}-i\varepsilon}\,\frac{i}{p_2^0+k^0-E_{2k}+i\varepsilon}\,\frac{1}{2E_{1k}\,2E_{2k}} \tag{2.19}$$

with E_{ik} defined in (2.17).

The same procedure will show that a ladder L_n with n rungs is obtained from the one with $n-1$ rungs as

$$L_n=L_{n-1}SL_1 \tag{2.20}$$

Summing over n and defining $L_0\equiv S$ we get the Dyson-Schwinger equation

$$L\equiv\sum_{n=0}^\infty L_n=S+L\,S\,L_1 \tag{2.21}$$

with a convolution on the rhs. as in (2.18). This is the Dyson-Schwinger equation for L with the lowest-order kernel L_1. Note that we did not need to specify the frame, the equation is valid for any e^+e^- momentum $P=p_1+p_2$.

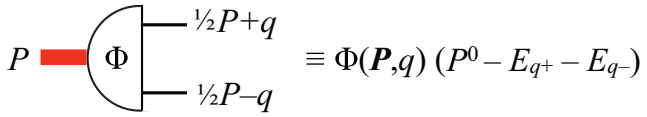

FIG. 5: A factor $P^0-E_{q+}-E_{q-}$ is included in the definition of the wave function, with $E_{q\pm}=\sqrt{(\frac12\boldsymbol P\pm\boldsymbol q)^2+m^2}$.

If the ladder sum L has a pole at $P^0=\sqrt{\boldsymbol P^2+M^2}$, with M the rest mass of the bound state, the residue will factorize as shown in Fig. 1 and (2.4). Canceling common factors on the two sides of (2.21) and expressing the wave function as indicated in Fig. 5 we find the Bethe-Salpeter equation (BSeq)

$$\begin{aligned} &\Phi(\boldsymbol P,q)(P^0-E_{q+}-E_{q-})=\\ &\qquad\sum_{\lambda_{int}}\int\frac{d^4k}{(2\pi)^4}\,\Phi(\boldsymbol P,k)(P^0-E_{k+}-E_{k-})S(\tfrac12P-k,\tfrac12P+k)L_1(\tfrac12P-k,\tfrac12P+k\to\tfrac12P-q,\tfrac12P+q) \end{aligned} \tag{2.22}$$

where S is given by (2.19) and $P^0=\sqrt{\boldsymbol P^2+M^2}$ (bound states are always "on-shell").

D. $\boldsymbol{P} = 0$: The Schrödinger equation

The Bethe-Salpeter equation (2.22) reduces to the Schrödinger equation in the rest frame, $\boldsymbol{P} = 0$. Using (2.6) the photon propagator of L_1 (2.14) is in Feynman gauge

$$D_{\mu\nu(q)} = \frac{ig_{\mu\nu}}{\boldsymbol{q}^2} \tag{2.23}$$

Due to the non-relativistic kinematics the upper (lower) components of the u (v) spinors dominate, hence the main contribution to L_1 is from the diagonal γ-matrix, *i.e.*, $\mu = \nu = 0$. The kernel of the BSeq (2.22)

$$L_1(\tfrac{1}{2}P - k, \tfrac{1}{2}P + k \to \tfrac{1}{2}P - q, \tfrac{1}{2}P + q) = -ie^2 \frac{4m^2}{(\boldsymbol{k} - \boldsymbol{q})^2} \tag{2.24}$$

is then independent of q^0 (and preserves helicities). The other factors on the rhs. of the BSeq also do not depend on q^0, consequently the wave function $\Phi(\boldsymbol{P} = 0, q)$ is independent of q^0. This implies that the wave function is an *equal-time* wave function: Doing the Fourier transform we find

$$\Phi(\boldsymbol{0}, \boldsymbol{q}; t_1, t_2) \equiv \int \frac{dq^0}{2\pi} e^{-i(\frac{1}{2}M + q^0)t_1 - i(\frac{1}{2}M - q^0)t_2} \Phi(\boldsymbol{0}, q) = \delta(t_1 - t_2) e^{-iMt} \Phi(\boldsymbol{0}, q) \tag{2.25}$$

with $t = t_1 = t_2$ the common time. This is a direct consequence of the fact that instantaneous Coulomb exchange dominates in the atomic rest frame. As we shall see, the situation is different for atoms with $\boldsymbol{P} \neq 0$.

In the integrand of the BSeq (2.22) only the propagator S depends on k^0,

$$\begin{aligned} \Phi(\boldsymbol{0}, \boldsymbol{q})(M - 2E_q) &= \int \frac{d^4k}{(2\pi)^4} \Phi(\boldsymbol{0}, \boldsymbol{k})(M - 2E_k) \frac{i}{-\frac{1}{2}M + k^0 + E_k - i\varepsilon} \frac{i}{\frac{1}{2}M + k^0 - E_k + i\varepsilon} \frac{-ie^2}{(\boldsymbol{k} - \boldsymbol{q})^2} \\ &= -e^2 \int \frac{d^3\boldsymbol{k}}{(2\pi)^3} \frac{\Phi(\boldsymbol{0}, \boldsymbol{k})}{(\boldsymbol{k} - \boldsymbol{q})^2} \end{aligned} \tag{2.26}$$

According to (2.6), $E_q \equiv \sqrt{\boldsymbol{q}^2 + m^2} \simeq m + \boldsymbol{q}^2/2m$ to leading order in α. Defining the binding energy E_B as in (2.5) we get the Schrödinger equation in momentum space,

$$\Big(E_B - \frac{\boldsymbol{q}^2}{2m_R}\Big)\Phi(\boldsymbol{0}, \boldsymbol{q}) = -4\pi\alpha \int \frac{d^3\boldsymbol{k}}{(2\pi)^3} \frac{\Phi(\boldsymbol{0}, \boldsymbol{k})}{(\boldsymbol{k} - \boldsymbol{q})^2} \tag{2.27}$$

where $m_R = \frac{1}{2}m$ is the reduced mass. In coordinate space,

$$\Phi(\boldsymbol{x}) \equiv \int \frac{d^3\boldsymbol{q}}{(2\pi)^3} \Phi(\boldsymbol{0}, \boldsymbol{q})\, e^{i\boldsymbol{q}\cdot\boldsymbol{x}} \tag{2.28}$$

the bound state equation (2.27) reads

$$\Big(-\frac{\boldsymbol{\nabla}^2}{2m_R} - \frac{\alpha}{|\boldsymbol{x}|}\Big)\Phi(\boldsymbol{x}) = E_B \Phi(\boldsymbol{x}) \tag{2.29}$$

E. $\boldsymbol{P} \neq 0$: Atoms in motion

The derivation of the bound state equation (2.22) in Section II C was based on summing Feynman diagrams. The Lorentz covariance of these diagrams allows to consider the frame dependence of atomic wave functions. The following discussion is based on the work by Matti Järvinen [12], and is instructive for understanding how bound states transform under Lorentz boosts. It is frequently assumed that bound states Lorentz contract similarly to the length of rods in classical relativity, therefore high-momentum protons and nuclei are depicted as ovals. We now learn that the situation is more involved in quantum physics.

1. Classical Lorentz contraction

Classical Lorentz contraction refers to a length measurement by two observers who are in relative motion. Each observer defines the length of a rod as the distance between its endpoints at an instant of time. The contraction arises

because the concept of simultaneity is frame dependent. We may assume that Observer A is at rest with the rod and that the frame of Observer B is reached by a boost ζ in the x-direction. If the endpoints of the rod are at $(0,0)$ and (t, L_A) in the rest frame they transform under the boost as

$$\begin{aligned}(0,0) &\rightarrow (0,0)\\ (t,L_A) &\rightarrow (t\cosh\zeta + L_A\sinh\zeta, t\sinh\zeta + L_A\cosh\zeta)\end{aligned} \tag{2.30}$$

Observer A measures the length of the rod at rest to be L_A, independently of the time t of his measurement. Observer B makes his measurement at time zero on his clock, *i.e.*, when

$$t\cosh\zeta + L_A\sinh\zeta = 0 \tag{2.31}$$

He thus finds the contracted length

$$L_B = t\sinh\zeta + L_A\cosh\zeta = \frac{L_A}{\cosh\zeta} \tag{2.32}$$

2. Equal-time wave functions

In atoms the ends of the rod correspond to the positions $\boldsymbol{x}_1$ and $\boldsymbol{x}_2$ of the electron and positron in the wave function (1.1). To study Lorentz contraction we need to consider *equal-time* wave functions, $x_1^0 = x_2^0$ in all frames. Such wave functions have a non-trivial, dynamic frame dependence – the relation was derived for the first time in [12]. The explicit covariance of the Bethe-Salpeter wave function in boosting the fermion fields relates wave functions defined at unequal times of the constituents ($x_1^0 \neq x_2^0$ in at least one of the frames).

States are defined by equal-time Fock state wave functions also in standard equal-time quantization, as given in (1.2). For positronium at rest only the $\phi_{e^+e^-}(\boldsymbol{x}_1, \boldsymbol{x}_2)$ wave function is non-vanishing at lowest order in α, and satisfies the Schrödinger equation (2.29) with $\boldsymbol{x} = \boldsymbol{x}_1 - \boldsymbol{x}_2$. As we shall see, also $\phi_{e^+e^-\gamma}$ is non-vanishing at lowest order when $\boldsymbol{P} \neq 0$.

3. Contribution from transversely polarized photon exchange

Let us then return to the lowest order bound state equation (2.22). In the rest frame $\boldsymbol{P} = 0$ analysis of the previous Section we made use of two simplifications:

1. The electrons moved non-relativistically, hence the upper (lower) components of the u (v) spinors were dominant. This allowed us to keep only Coulomb photon exchange ($\mu = \nu = 0$) in the kernel L_1 of (2.14) and Fig. 4(a).
2. According to (2.6) the exchanged energy q^0 could be neglected compared to the three-momentum $\boldsymbol{q}$.

Neither of these assumptions is valid for a general bound state momentum $\boldsymbol{P}$. The vertex factors $\bar{v}\gamma^\mu v$ and $\bar{u}\gamma^\mu u$ in (2.14) transform as 4-vectors and reduce to $2m\, g^{\mu 0} \simeq P^\mu$ in the rest frame. Hence helicity is conserved in any frame and

$$\bar{u}(\tfrac{1}{2}P + q)\gamma^\mu u(\tfrac{1}{2}P + k) = \bar{v}(\tfrac{1}{2}P - k)\gamma^\mu v(\tfrac{1}{2}P - q) \simeq P^\mu \tag{2.33}$$

In Coulomb gauge the photon propagator is,

$$D^{00}(q) = \frac{i}{\boldsymbol{q}^2} \qquad D^{0j}(q) = D^{j0}(q) = 0 \qquad D^{jk}(q) = \frac{i}{q^2}\Big(\delta^{jk} - \frac{q^j q^k}{\boldsymbol{q}^2}\Big) \tag{2.34}$$

The transverse part $D^{jk}(q^0, \boldsymbol{q})$ depends on q^0, and hence (after a Fourier transform) $D^{jk}(t, \boldsymbol{q})$ depends on t: Transverse photons propagate in time. When the transverse photon is in flight the equal-time Fock state will thus be $|e^+e^-\gamma\rangle$, and will be described by the separate wave function $\phi_{e^+e^-\gamma}$.

It is perhaps worthwhile to convince ourselves with the help of a simple example that the transverse photon contribution cannot be neglected. Let us compare the rest frame expression for the $2 \to 2$ amplitude (Fig. 6) with that in a general frame. For simplicity we may assume the charged particles to be scalars, and assume 90° scattering in the CM:

$$\tfrac{1}{2}P = (m\sqrt{1+\alpha^2}, \boldsymbol{0}) \qquad k = (0,0,0,\alpha m) \qquad q = (0, \alpha m, 0, 0) \tag{2.35}$$

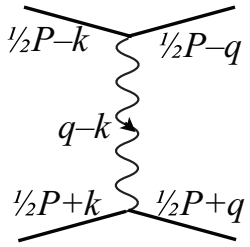

FIG. 6: Single photon exchange amplitude A. The charged particles are taken to be scalars.

Using Feynman gauge the Lorentz invariant full amplitude is easily found to be

$$A = 4\pi\,\frac{2+3\alpha^2}{\alpha} \tag{2.36}$$

After a boost ζ in the z-direction the momenta (2.35) are

$$\tfrac{1}{2}P = m\sqrt{1+\alpha^2}(\cosh\zeta, 0, 0, \sinh\zeta) \qquad k = \alpha m(\sinh\zeta, 0, 0, \cosh\zeta) \qquad q = (0, \alpha m, 0, 0) \tag{2.37}$$

The propagator (2.34) contributes a Coulomb (C) and transverse (T) part to the scattering amplitude,

$$A_C = \frac{4\pi}{\alpha}\,\frac{(4+3\alpha^2)\cosh^2\zeta + \alpha^2}{\cosh^2\zeta + 1} \qquad A_T = -\frac{8\pi}{\alpha}\,\frac{\sinh^2\zeta - \alpha^2}{\cosh^2\zeta + 1)} \tag{2.38}$$

which together form the full amplitude of (2.36), $A = A_C + A_T$. In the CM ($\zeta = 0$) the leading contribution to A is from A_C for small α, but in a general frame A_C and A_T are comparable.

The q^0-dependence of the transverse propagator in the kernel L_1 of the bound state equation (2.22) implies that $\Phi(\boldsymbol{P}, q)$ depends on q^0, *i.e.*, $\Phi(\boldsymbol{P}, k)$ depends on k^0. Hence in this form the integral equation cannot be easily reduced to a time-independent equation, as was the case in the rest frame. This reflects the fact that there are intermediate states with propagating, transverse photons.

4. Time ordering

In a time-ordered description the "life-time" of each intermediate state is inversely proportional to its difference in energy compared to the initial state. The energies of $|e^+e^-\rangle$ Fock states differ from the positronium energy by approximately the binding energy, and thus are of $\mathcal{O}\left(\alpha^2\right)$ (in any frame). The energy of a transverse photon with bound state momentum $\boldsymbol{q}$ of $\mathcal{O}\left(\alpha m\right)$ in the rest frame is $E_q = |\boldsymbol{q}|$ and remains of $\mathcal{O}\left(\alpha\right)$ in any frame[4]. At small α the positronium atom propagates most of the time as an $|e^+e^-\rangle$ Fock state, with only an $\mathcal{O}\left(\alpha\right)$ probability to find a transverse photon in flight. While the scattering amplitude (2.38) showed that this contribution nevertheless cannot be neglected, the probability that *two* transverse photons are in flight simultaneously is of $\mathcal{O}\left(\alpha\right)$. Similarly the contribution where an instantaneous Coulomb photon is exchanged during the flight of a transverse photon can be neglected at lowest order.

Multiple, overlapping photon exchanges do contribute at higher orders. This is one of the aspects that complicate bound state perturbation theory. For example, the vertex correction in Fig. 4(d) contributes to the Lamb shift at $\mathcal{O}\left(\alpha^5\right)$. At this order any number of Coulomb exchanges may be exchanged while the transverse photon is in flight. To find the Dirac equation by summing Feynman diagrams we must likewise include diagrams with any number of overlapping photon exchanges.

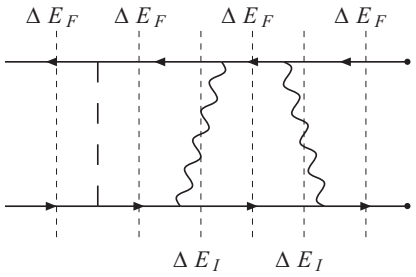

FIG. 7: Positronium propagates mostly as an e^+e^- state (time slices are indicated by the short dashed lines). Transverse photons are exchanged only $\mathcal{O}\left(\alpha\right)$ of the time, since $\Delta E_F \propto \alpha^2$ while $\Delta E_I \propto \alpha$. Contributions with overlapping photon exchanges may be neglected at lowest order. Figure from [19].

We now take advantage of the non-overlapping photon exchanges for positronium by time-ordering the bound state equation (2.22). The equal-time e^+e^- wave function $\phi_{e^+e^-} \equiv \Phi(\boldsymbol{P}, \boldsymbol{q})$ is defined by the Fourier transform,

$$\begin{aligned}\Phi(\boldsymbol{P}, t, \boldsymbol{q}) &= \int \frac{dq^0}{2\pi}\Phi(\boldsymbol{P}, q^0, \boldsymbol{q})\, e^{-it(\frac{1}{2}P^0+q^0)-it(\frac{1}{2}P^0-q^0)} \\ &= e^{-itP^0}\int \frac{dq^0}{2\pi}\Phi(\boldsymbol{P}, q^0, \boldsymbol{q}) \equiv e^{-itP^0}\Phi(\boldsymbol{P}, \boldsymbol{q})\end{aligned} \tag{2.39}$$

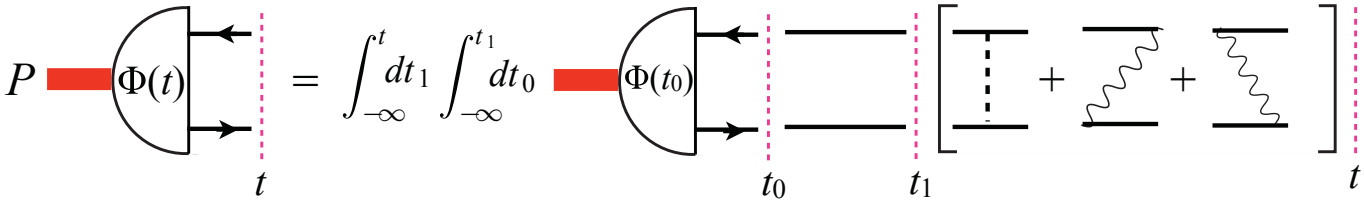

FIG. 8: Time-ordered version of the bound state equation (2.22): $\Phi = \Phi\, S\, L_1$.

[4] Recall that in a time ordered picture all particles are treated as "on-shell".

The time ordering of the propagators S in (2.19) is, for $t > 0$ and with $E_{k\pm} = \sqrt{(\frac{1}{2}\boldsymbol{P} \pm \boldsymbol{k})^2 + m^2}$,

$$S_f(t, \tfrac{1}{2}\boldsymbol{P} + \boldsymbol{k}) = \int \frac{dk^0}{2\pi} \frac{ie^{-it(\frac{1}{2}P^0 + k^0)}}{\frac{1}{2}P^0 + k^0 - E_{k+} + i\varepsilon} = e^{-itE_{k+}}$$

$$S_{\bar{f}}(t, \tfrac{1}{2}\boldsymbol{P} - \boldsymbol{k}) = \int \frac{dk^0}{2\pi} \frac{ie^{-it(\frac{1}{2}P^0 - k^0)}}{-\frac{1}{2}P^0 + k^0 + E_{k-} - i\varepsilon} = -e^{-itE_{k-}} \tag{2.40}$$

The time-ordered then takes the form indicated in Fig. 8,

$$\Phi(\boldsymbol{P}, t, \boldsymbol{q}) = \int_{-\infty}^{t} dt_1 \int_{-\infty}^{t_1} dt_0 \int \frac{d^3\boldsymbol{k}}{(2\pi)^3} \Phi(\boldsymbol{P}, t_0, \boldsymbol{k}) S(t_1 - t_0) L_1(t - t_1) \tag{2.41}$$

The time-ordered kernel $L_1(t - t_1)$ has contributions from instantaneous Coulomb exchange $\propto \delta(t - t_1)$ and from the transverse photon propagator in (2.34). The Fourier transform of the factor $1/q^2$ in the transverse photon propagator has as, in (2.2), two contributions, depending on whether the photon propagates forward or backward in time. Using (2.33) for the vertex factors the bound state equation becomes

$$e^{-itP^0}\Phi(\boldsymbol{P}, \boldsymbol{q})(P^0 - E_{q+} - E_{q-}) = \int \frac{d^3\boldsymbol{k}}{(2\pi)^3} \int_{-\infty}^{t} dt_1 \int_{-\infty}^{t_1} dt_0\, e^{-it_0 P^0} \Phi(\boldsymbol{P}, \boldsymbol{k})(P^0 - E_{k+} - E_{k-})$$

$$\times \frac{-1}{2E_{k+}2E_{k-}} e^{-i(t_1 - t_0)(E_{k+} + E_{k-})} \tag{2.42}$$

$$\times(-ie^2)\left\{ i\frac{(P^0)^2}{(\boldsymbol{q} - \boldsymbol{k})^2}\delta(t - t_1) + \left[\boldsymbol{P}^2 - \frac{\big(\boldsymbol{P} \cdot (\boldsymbol{q} - \boldsymbol{k})\big)^2}{(\boldsymbol{q} - \boldsymbol{k})^2}\right] \frac{e^{-i(t-t_1)(E_{k-} + E_{q+} + |\boldsymbol{q} - \boldsymbol{k}|)} + e^{-i(t-t_1)(E_{k+} + E_{q-} + |\boldsymbol{q} - \boldsymbol{k}|)}}{2|\boldsymbol{q} - \boldsymbol{k}|} \right\}$$

When the time integrals are done we have a bound state equation for the equal-time wave function of the $|e^+e^-\rangle$ Fock state,

$$\Phi(\boldsymbol{P}, \boldsymbol{q})(P^0 - E_{q+} - E_{q-}) = -e^2 \int \frac{d^3\boldsymbol{k}}{(2\pi)^3} \Phi(\boldsymbol{P}, \boldsymbol{k}) \frac{1}{2E_{k+}2E_{k-}} \tag{2.43}$$

$$\times \left\{ \frac{(P^0)^2}{(\boldsymbol{q} - \boldsymbol{k})^2} + \frac{1}{2|\boldsymbol{q} - \boldsymbol{k}|}\left[\frac{1}{P^0 - E_{k-} - E_{q+} - |\boldsymbol{q} - \boldsymbol{k}|} + \frac{1}{P^0 - E_{k+} - E_{q-} - |\boldsymbol{q} - \boldsymbol{k}|}\right]\left[\boldsymbol{P}^2 - \frac{\big(\boldsymbol{P} \cdot (\boldsymbol{q} - \boldsymbol{k})\big)^2}{(\boldsymbol{q} - \boldsymbol{k})^2}\right] \right\}$$

This equation has no obvious Lorentz covariance. Thus it is not clear that the energy eigenvalue P^0 has the frame dependence required by Lorentz symmetry, nor whether the wave function Lorentz contracts. We shall now verify these properties in the range of validity of the equation, *i.e.*, at lowest order in α.

5. Reduction to the Schrödinger equation

Let us first identify the leading power of α on both sides of the equation. On the lhs. $P^0 - E_{q+} - E_{q-}$ is of the order of the binding energy, hence of $\mathcal{O}\left(\alpha^2\right)$. On the rhs. the (boosted) Bohr momenta $|\boldsymbol{k}|, |\boldsymbol{q}| \propto \alpha$. Hence in the numerator $e^2 \int d^3\boldsymbol{k} \propto \alpha^4$ while in the denominator $(\boldsymbol{q} - \boldsymbol{k})^2 \propto \alpha^2$. The leading powers of α agree, and subleading powers may be ignored.

We denote the electron energy at zeroth order in α by E,

$$E = \sqrt{(\tfrac{1}{2}\boldsymbol{P})^2 + m^2} \tag{2.44}$$

The binding energy E_B is defined in accordance with (2.5),

$$P^0 = \sqrt{\boldsymbol{P}^2 + (2m + E_B)^2} = 2E + \frac{m}{E} E_B + \mathcal{O}\left(\alpha^2\right) \equiv 2E + \frac{1}{\gamma} E_B \qquad \gamma = \frac{E}{m} \tag{2.45}$$

where γ is the usual Lorentz factor at zeroth order in α. The electron energy up to $\mathcal{O}\left(\alpha^2\right)$ is

$$E_{q+} = \sqrt{(\tfrac{1}{2}\boldsymbol{P} + \boldsymbol{q})^2 + m^2} = E + \frac{1}{2E}\, \boldsymbol{q} \cdot (\boldsymbol{P} + \boldsymbol{q}) - \frac{1}{8E^3} (\boldsymbol{q} \cdot \boldsymbol{P})^2 + \mathcal{O}\left(\alpha^3\right) \tag{2.46}$$

The factor on the lhs. of (2.43) is then

$$(P^0 - E_{q+} - E_{q-}) = \frac{1}{E}\left(mE_B - q_\perp^2 - \frac{1}{\gamma^2}\, q_\parallel^2\right) + \mathcal{O}\left(\alpha^3\right) \qquad \boldsymbol{P}\cdot\boldsymbol{q} \equiv |\boldsymbol{P}|\, q_\parallel \tag{2.47}$$

where we defined the $\parallel$ and $\perp$ directions wrt. $\boldsymbol{P}$. The energy denominators in (2.43) are

$$\begin{aligned} P^0 - E_{k-} - E_{q+} - |\boldsymbol{q}-\boldsymbol{k}| &= \frac{1}{P^0}\,\boldsymbol{P}\cdot(\boldsymbol{k}-\boldsymbol{q}) - |\boldsymbol{q}-\boldsymbol{k}| + \mathcal{O}\left(\alpha^2\right) \\ P^0 - E_{k+} - E_{q-} - |\boldsymbol{q}-\boldsymbol{k}| &= -\frac{1}{P^0}\,\boldsymbol{P}\cdot(\boldsymbol{k}-\boldsymbol{q}) - |\boldsymbol{q}-\boldsymbol{k}| + \mathcal{O}\left(\alpha^2\right) \end{aligned} \tag{2.48}$$

so that

$$\frac{1}{P^0 - E_{k-} - E_{q+} - |\boldsymbol{q}-\boldsymbol{k}|} + \frac{1}{P^0 - E_{k+} - E_{q-} - |\boldsymbol{q}-\boldsymbol{k}|} = \frac{(P^0)^2}{(\boldsymbol{q}-\boldsymbol{k})^2}\,\frac{-2|\boldsymbol{q}-\boldsymbol{k}|}{\boldsymbol{P}^2 - \frac{\left(\boldsymbol{P}\cdot(\boldsymbol{q}-\boldsymbol{k})\right)^2}{(\boldsymbol{q}-\boldsymbol{k})^2} + 4m^2}\Big[1 + \mathcal{O}\left(\alpha^2\right)\Big] \tag{2.49}$$

Substituting this in (2.43) and noting that $2E_{k+}2E_{k-} \simeq (P^0)^2$ the bound state equation becomes

$$\Phi(\boldsymbol{P},\boldsymbol{q})\left(mE_B - q_\perp^2 - \frac{1}{\gamma^2}\, q_\parallel^2\right) = -\frac{e^2 m}{\gamma}\int \frac{d^3\boldsymbol{k}}{(2\pi)^3}\,\frac{\Phi(\boldsymbol{P},\boldsymbol{k})}{(\boldsymbol{q}-\boldsymbol{k})_\perp^2 - \frac{1}{\gamma^2}(\boldsymbol{q}-\boldsymbol{k})_\parallel^2} \tag{2.50}$$

This is the same as the rest frame equation (2.27) when the longitudinal components of $\boldsymbol{q}$ and $\boldsymbol{k}$ are scaled by γ. We conclude that the binding energy E_B is independent of $\boldsymbol{P}$, so that the energy (2.45) of the bound state has the correct frame dependence. The wave function Lorentz contracts classically in coordinate space since the longitudinal component of all relative momenta scale with the Lorentz factor γ.

The wave function $\phi_{e^+e^-\gamma}$ of the $|e^+e^-\gamma\rangle$ Fock component is given by the sum of the amplitudes for the radiation of the photon from the electron and the positron [12]. With increasing bound state momentum $\boldsymbol{P}$ the photon is emitted preferentially in the forward direction (and hence does not simply contract). In the infinite momentum frame the result agrees with the wave function of Light-Front quantization.

An equal-time formulation thus allows to study bound states both in the rest frame (with rotational symmetry) and in the infinite momentum frame (where the momentum gives a preferred direction). When the Coulomb field of the rest frame is boosted it generates a transverse field component. The underlying Poincaré invariance of QED ensures that all physical quantities have the correct frame dependence, even though equal-time wave functions transform non-trivially under boosts.

---

[1] E. E. Salpeter and H. A. Bethe, Phys. Rev. **84** (1951) 1232.

[2] J. R. Sapirstein and D. R. Yennie, *"Theory of Hydrogenic Bound States",* in *Quantum Electrodynamics,* edited by T. Kinoshita (World Scientific, Singapore, 1990), p. 560 [http://inspirehep.net/record/27093?ln=en].

[3] G. P. Lepage, Phys. Rev. A **16** (1977) 863;
W. E. Caswell and G. P. Lepage, Phys. Rev. A **18** (1978) 810;
G. P. Lepage, SLAC-0212 (1978) [http://www.slac.stanford.edu/pubs/slacreports/slac-r-212.html].

[4] W. E. Caswell and G. P. Lepage, Phys. Lett. B **167** (1986) 437 [http://inspirehep.net/record/213093?ln=en].

[5] T. Kinoshita and G. P. Lepage, *"Quantum Electrodynamics for Nonrelativistic Systems and High Precision Determinations of alpha",* in *Quantum Electrodynamics,* edited by T. Kinoshita (World Scientific, Singapore, 1990), p. 81 [http://inspirehep.net/record/28117?ln=en];
T. Kinoshita, hep-ph/9808351.

[6] A. Czarnecki, Acta Phys. Polon. B **30** (1999) 3837 [hep-ph/9911455].

[7] M. W. Ritter, P. O. Egan, V. W. Hughes and K. A. Woodle, Phys. Rev. **A30** (1984) 1331.

[8] C. D. Roberts, arXiv:1203.5341 [nucl-th].

[9] N. Brambilla, A. Pineda, J. Soto and A. Vairo, Rev. Mod. Phys. **77** (2005) 1423 [hep-ph/0410047].

[10] Z. Fodor, PTEP **2012** (2012) 01A108.

[11] Figure adapted from a presentation of J. Ritman at the *Workshop on QCD in Nuclear and Hadronic Physics* at CCLRC Daresbury Laboratory on 3 - 4 March 2005, `http://npg.dl.ac.uk/QCD/`.

[12] M. Järvinen, Phys. Rev. D **71** (2005) 085006 [arXiv:hep-ph/0411208].

[13] S. J. Brodsky, Atomic Physics and Astrophysics, Vol. I, edited by M. Chretien and E. Lipworth (Gordon and Breach Science, New York), p. 91 (1969);
F. Gross, Phys. Rev. C **26** (1982) 2203;
A. R. Neghabian and W. Gloeckle, Can. J. Phys. **61** (1983) 85.

[14] M. S. Plesset, Phys. Rev. **41** (1932) 278.

[15] F. J. Dyson, Phys. Rev. **85** (1952) 631.

[16] J. Iliopoulos, C. Itzykson and A. Martin, Rev. Mod. Phys. **47** 165 (1975);
C. Itzykson and J.-B. Zuber, *Quantum Field Theory* (McGraw-Hill, New York, 1980), Sec. 6-2-1.

[17] S. J. Brodsky and P. Hoyer, Phys. Rev. D **83** (2011) 045026 [arXiv:1009.2313 [hep-ph]].
[18] B. R. Holstein and J. F. Donoghue, Phys. Rev. Lett. **93**, 201602 (2004) [hep-th/0405239].
[19] M. Järvinen, *Spin and Relativistic Motion of Bound States*, PhD thesis (2007), http://urn.fi/URN:ISBN:978-952-10-3250-9.